

Title	Element dependence of local disorder in medium- entropy alloy CrCoNi
Author(s)	Hanasaki, N.; Oda, M.; Niitsu, K. et al.
Citation	AIP Advances. 2021, 11(12), p. 125216
Version Type	VoR
URL	https://hdl.handle.net/11094/103016
rights	Copyright 2021 Authors. This article is distributed under a Creative Commons Attribution (CC BY) License.
Note	

### The University of Osaka Institutional Knowledge Archive : OUKA

https://ir.library.osaka-u.ac.jp/

The University of Osaka

RESEARCH ARTICLE | DECEMBER 15 2021

## Element dependence of local disorder in medium-entropy alloy CrCoNi

N. Hanasaki 🗖 📵 ; M. Oda; K. Niitsu 📵 ; K. Ehara; H. Murakawa; H. Sakai 📵 ; H. Nitani; H. Abe 🗓 ; H. Saqayama; H. Uetsuka; T. Karube; H. Inui



AIP Advances 11, 125216 (2021) https://doi.org/10.1063/5.0072766





#### Articles You May Be Interested In

Local structural disorder introduced by Cr in fcc high-/medium-entropy alloys consisting of 3d transition metal elements

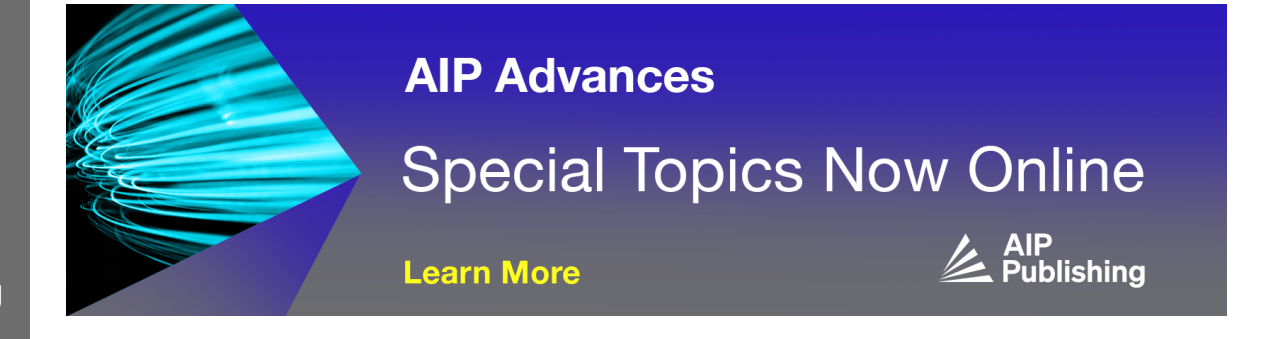
Appl. Phys. Lett. (November 2024)

Martensitic transformation in CrCoNi medium-entropy alloy at cryogenic temperature

Appl. Phys. Lett. (September 2021)

Atomic displacement in the CrMnFeCoNi high-entropy alloy – A scaling factor to predict solid solution strengthening

AIP Advances (December 2016)





# Element dependence of local disorder in medium-entropy alloy CrCoNi

Cite as: AIP Advances 11, 125216 (2021); doi: 10.1063/5.0072766 Submitted: 6 October 2021 • Accepted: 18 November 2021 • Published Online: 15 December 2021







N. Hanasaki,<sup>1,a)</sup> M. Oda,<sup>1</sup> K. Niitsu,<sup>2,3</sup> K. Ehara,<sup>2</sup> H. Murakawa,<sup>1</sup> H. Sakai,<sup>1</sup> H. Nitani,<sup>4</sup> H. Abe,<sup>4,5,6</sup> H. Sagayama,<sup>4</sup> H. Uetsuka,<sup>7</sup> T. Karube,<sup>7</sup> and H. Inui<sup>2,3</sup>

#### **AFFILIATIONS**

- <sup>1</sup>Department of Physics, Osaka University, Toyonaka, Osaka 560-0043, Japan
- <sup>2</sup>Department of Materials Science and Engineering, Kyoto University, Kyoto 606-8501, Japan
- <sup>3</sup>Center for Elements Strategy Initiative for Structure Materials (ESISM), Kyoto University, Kyoto 606-8501, Japan
- <sup>4</sup>Institute of Materials Structure Science, High Energy Accelerator Research Organization (KEK), 1-1 Oho, Tsukuba, Ibaraki 305-0801, Japan
- <sup>5</sup>Department of Materials Structure Science, School of High Energy Accelerator Science, SOKENDAI (The Graduate University for Advanced Studies), 1-1 Oho, Tsukuba, Ibaraki 305-0801, Japan
- Graduate School of Science and Engineering, Ibaraki University, 2-1-1 Bunkyo, Mito, Ibaraki 310-8512, Japan
- <sup>7</sup>Asahi Diamond Industrial Co., Ltd., Kawasaki, Kanagawa 213-0032, Japan

#### **ABSTRACT**

The medium-entropy alloy CrCoNi is known to have exceptional mechanical properties. To clarify its local structure, we performed extended x-ray absorption fine structure measurement of CrCoNi. The structural disorder is larger in Cr sites than in other constituent elements, which is consistent with the larger atomic displacement of the Cr atoms predicted by previous first-principles calculations. The Cr atom has a solute-type characteristic that induces local disorder. The differences in local disorder among the constituent elements decrease as the annealing time increases in the temperature range in which a short-range order develops.

© 2021 Author(s). All article content, except where otherwise noted, is licensed under a Creative Commons Attribution (CC BY) license (http://creativecommons.org/licenses/by/4.0/). https://doi.org/10.1063/5.0072766

High/medium-entropy alloys (H/MEAs), also referred to as multiprincipal element alloys, have attracted a great deal of attention because of their exceptional mechanical properties.<sup>1,2</sup> Their high fracture toughness was reported even at cryogenic temperatures.3 In traditional alloys, solute atoms are dissolved in the solvent matrix and prevent dislocation motion. Since solvent and solute atoms cannot be well defined in equiatomic alloys, the concept of the traditional solid-solution strengthening model is not applicable to H/MEAs.<sup>4,5</sup> Several theoretical explanations of their high strength have been proposed so far. Toda-Caraballo et al. discussed lattice distortion due to different local combinations of constituent elements by extending the conventional theory of binary systems.<sup>6</sup> Varenne et al. considered the effective medium of a multicomponent matrix approximately and calculated the interaction with the dislocation.7 Okamoto et al. pointed out that the yield strength normalized by the shear modulus is correlated with the mean-square

atomic displacement (MSAD). These atomic displacements depend largely on the constituent elements, and Cr atoms tend to have larger atomic displacements. A constituent element with a larger atomic displacement induces a structural local disorder. Such an element can be considered a "solute-type" (guest-type) element. On the other hand, a constituent element having a smaller atomic displacement can be regarded a "solvent-type" (host-type) element that matches the lattice structure. To clarify the mechanism for the high strength of H/MEAs, it is important to investigate the local structure experimentally and to distinguish the characteristics of each constituent element.

Extended x-ray absorption fine structure (EXAFS) spectroscopy is a powerful probe for site-selective local structure analysis. <sup>10,11</sup> By estimating the Debye–Waller factors in the constituent elements, we can reveal how the local structure is disordered around each element. Recently, the relationship between short-range

a) Author to whom correspondence should be addressed: hanasaki@phys.sci.osaka-u.ac.jp

order and hardening has also been discussed. 12 The development of short-range order is influenced by heat treatment. In general, at higher temperatures, a random configuration of constituent elements tends to occur. The chemical short-range order is promoted by low-temperature annealing.<sup>13</sup> Unfortunately, the heat-treatment effect on the lattice structure is still unclear experimentally. In this paper, we used EXAFS measurement to examine the effects of annealing on the local structure of CrCoNi, which has the highest yield strength at cryogenic temperatures among a class of fcc-type single-phase MEAs composed of Cr, Mn, Fe, Co, and Ni. To detect the static local structure, we measured the EXAFS at the lowest temperatures at which the thermal fluctuation of the lattice is suppressed. A CrCoNi crystal was synthesized in a floating zone furnace and homogenized at 1473 K for 24 h. The ingot was crushed into powder. The powder was subjected to short-term (5 min) annealing at 1473 K to remove any strains and/or defects introduced during powderization. To change the degree of short-range order, the powders were additively annealed at 773 and 1123 K. All the heat treatments were carried out in vacuo, and then, the powders were quenched in water. The obtained powders were pressed with boron nitride into a pellet. We performed the EXAFS measurement using a BL-12C and by x-ray diffraction using a BL-8B at the KEK Photon Factory. Transmission mode was adopted to obtain high measurement precision. The obtained spectra were analyzed by Athena and Artemis software.14

Figure 1(a) shows an example of the EXAFS function of  $k^2$ weighted  $\chi$  (k), which was measured at the K edges of Cr, Co, and Ni in CrCoNi annealed at 773 K for 20 h. Here, the wave number k was calculated by  $E - E_0 = \hbar^2 k^2 / 2m$ , where  $E_0$  and m denote the energies of the K absorption edges of Cr, Co, and Ni, and the electron mass, respectively. From the Fourier transform in Fig. 1(a), the radial distribution function was obtained, as shown in Fig. 1(b). The peaks near  $r_{\text{EXAFS}} = 2.2 \text{ Å correspond to the pair correlation between}$ the x-ray absorbing atom and the nearest neighbor atom in the fcc structure, as indicated by (1) in the inset of the figure. The peaks near  $r_{\text{EXAFS}} = 3.4$ , 4.0, and 4.7 Å show the pairs of the second, third, and fourth nearest neighbor atoms of the fcc structure, respectively. It should be noted that the peak position shown in Fig. 1(b) deviates from the actual distance of atomic pairs owing to the phase shift. The actual distance between the x-ray absorbing atom and the nearest neighbor atom is estimated to be r = 2.49-2.52 Å. To focus on the nearest neighbor atoms, we analyzed the EXAFS function obtained by the inverse Fourier transform in the range of  $r_{\text{EXAFS}} = 1-3 \text{ Å}$  in

Figure 2(a) displays the annealing-temperature dependence of the Debye–Waller factors obtained by the EXAFS in the Cr, Co, and Ni K edges. The right, middle, and left data correspond to the samples annealed at 1473 K for 5 min, 1123 K for 2 h, and 773 K for 2 h, respectively. After high-temperature annealing, Cr, Co, and Ni atoms are expected to exist randomly near the lattice points, as suggested by molecular dynamics simulations. Thus, in estimating the Debye–Waller factors in the nearest neighbor atoms, we assumed an averaged configuration of Cr, Co, and Ni around the x-ray absorbing atom as a first approximation. The assumed element configuration has an influence on the estimated value of the Debye–Waller factors. If the x-ray absorbing atom is surrounded by Ni (Cr), the Debye–Waller factor increases by  $|\Delta\sigma^2| < 0.0004 \text{ Å}^2$  (decreases by  $|\Delta\sigma^2| < 0.0004 \text{ Å}^2$  (decreases by  $|\Delta\sigma^2| < 0.0004 \text{ Å}^2$ ). The difference in the Debye–Waller factors

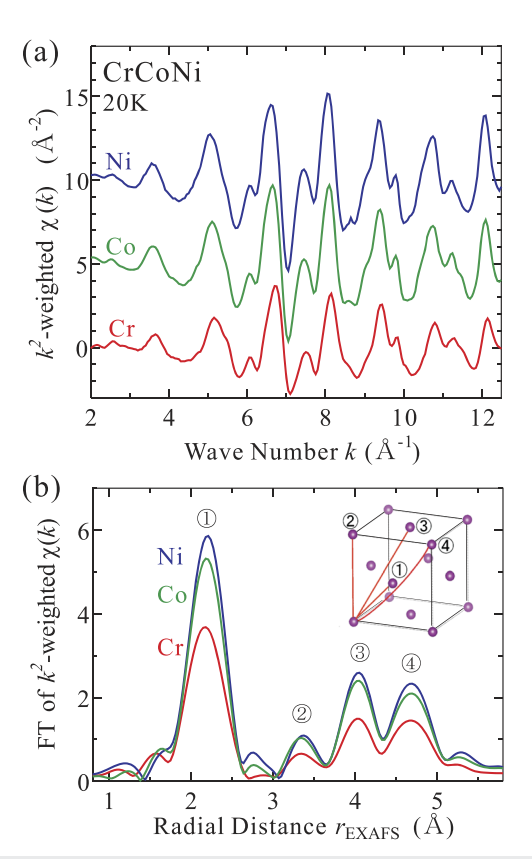


**FIG. 1.** (a) Extended x-ray absorption fine structure (EXAFS)  $k^2$ -weighted  $\chi(k)$  measured at 20 K in Cr (red), Co (green), and Ni (blue) K edges in CrCoNi annealed at 773 K for 20 h. As an aid to the eye, each spectrum is offset by 5. (b) Radial distribution function obtained by the Fourier transform of (a). The peak near  $r_{\rm EXAFS} = 2.2$  Å is ascribed to the correlation between the x-ray absorbing atom and the nearest neighbor atoms. The inset illustrates the correspondence between the peaks in (b) and the pair correlation in the fcc structure.

between Cr and Ni shown in Fig. 2(a) is larger than the possible change in the Debye–Waller factors given by the element configurations that are different from the averaged one. Therefore, the local disorder concerning the atomic positions around Cr is larger than that around Ni. The Cr atom does not match the lattice structure and is considered a solute-type atom disturbing the lattice structure. This is consistent with the report that high residual resistivity was observed in equiatomic alloys containing the Cr atoms. <sup>18</sup> On the other hand, the Ni atom can be regarded as a solvent-type atom matching the lattice. By the low-temperature heat treatment, the Debye–Waller factor of the Ni sites tends to decrease slightly.

The first-principles calculation suggests that the MSAD depends largely on the element. <sup>8,19</sup> In CrCoNi, it is theoretically suggested that the Cr, Co, and Ni atoms have the largest, the intermediate, and the smallest MSADs (0.0061, 0.0023, and 0.0012 Å<sup>2</sup>), respectively. <sup>9</sup> If the x-ray absorbing atom is displaced, the difference in the distances between this absorbing atom and the nearest neighbor atoms is made. The photoelectron wave emitted from the x-ray absorbing atom is scattered by the surrounding atoms. The phase of the returning wave becomes different from those scattered by other

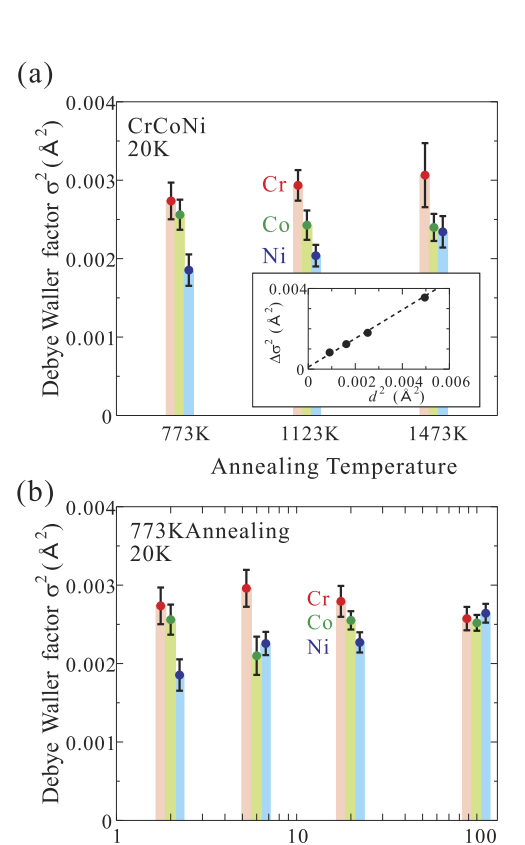


**FIG. 2.** (a) Dependence of the Debye–Waller factors obtained by EXAFS in Cr (red), Co (green), and Ni (blue) of CrCoNi at annealing temperature. Annealing at 1123 and 773 K for 2 h is performed after heat treatment at 1473 K for 5 min for homogenization. The Debye–Waller factors are estimated using the data measured at 20 K. Inset: Calculated relationship between the increment in the Debye–Waller factor  $\Delta\sigma^2$  and the square of the atomic displacement  $d^2$ . The dashed line is a guide for the eye. (b) Annealing-time dependence of the Debye–Waller factor on the annealing at 773 K after heat treatment at 1473 K. For clarity, the data in each element are shifted slightly in the horizontal direction.

Annealing Time (hours)

nearest neighbor atoms, leading to the decay of the photoelectron wave. The Debye-Waller factor increases as a result. To consider the effect of atomic displacement, we calculated the Debye-Waller factors on the assumption that the x-ray absorbing atom is displaced from the ideal lattice position. As seen in the inset of Fig. 2(a), the increment in the Debye-Waller factor  $\Delta \sigma^2$  has the same order as the square of the atomic displacement  $d^2$ , and  $\Delta \sigma^2$  is nearly proportional to  $d^2$ . The experimental result that the Debve-Waller factor in the Cr site is larger than that in the Ni site is qualitatively consistent with the atomic displacement predicted by the first-principles calculation in CrCoNi. It is also reported that the Cr atoms tend to have the largest atomic displacement in many other H/MEAs, such as CrMnFeCoNi. 8,9 It is reasonable to consider that Cr displacement plays a major role in the mechanical properties of H/MEAs and contributes to the random spatial fluctuation of the atomic positions. This fluctuation is most likely to cause an effective anchor that prevents the dislocation motion. Transition-metal atoms having low valence-electron numbers, such as Cr atoms, tend to form the bcc structure.<sup>9</sup> This might be the reason why the Cr atom has the largest displacement in the fcc structure.

The molecular dynamics simulation also suggests that the configurational entropy decreases as the chemical short-range order grows below ~1000 K.<sup>13</sup> The electron transmission microscopy measurement supports that long-term annealing followed by slow cooling promotes the growth of the short-range order. 12 Unfortunately, it is difficult to determine the element configuration around the x-ray absorbing atom in the short-range order by EXAFS measurement since the differences in the backscattering effect of the photoelectron between Cr, Co, and Ni are small.<sup>15</sup> However, we can investigate the influence of the short-range order on the local disorder. Figure 2(b) shows the Debye-Waller factors in various annealing times at 773 K. Since the K edge in Co is close to that in Ni, the energy range analyzed in Co is narrower than that in Cr and Ni. The measurement precision of the Debye-Waller factor in Co is not as high as that in Cr and Ni. As the annealing time increased, the differences in the Debye-Waller factors among the constituent elements decreased gradually. After 100 h of annealing, the Debye-Waller factors in all of the constituent elements were close to each other. The first-principles calculation suggests that in the low-temperature annealing, the element configuration is locally optimized by the interaction between the elements, leading to the growth of the local order. 13 The displacement of each atom is determined by the detailed balance between the interactions with the surrounding elements in the local order and thus is no longer a characteristic of each element. According to Zhang et al., 12 the development of the shortrange order results in an increase in the local strain. Accordingly, the change in the Debye-Waller factor upon annealing is a result of the collaborative atomic displacement inside the strained regions. Although EXAFS measurement does not allow us to figure out the microstructural features in real space, this result is likely to capture the change in the local strain state, which plays an important role in determining the mechanical properties.

Yield strength decreases at higher temperatures.<sup>20</sup> To reveal the correlation between yield strength and local disorder, we measured the temperature dependence of the Debye-Waller factors on CrCoNi annealed at 773 K for 20 h, as shown in Fig. 3. The Debye-Waller factors reported in pure metal Cr and Ni have temperature dependence similar to that in CrCoNi (Fig. S1 in the supplementary material).<sup>21</sup> At the lowest temperature, 20 K, the Debye-Waller factors indicate local static disorder. The values of these factors increase at temperatures above ~77 K since the phonon is thermally excited.<sup>22</sup> Since the ratio of the contribution of the thermally excited phonon at 20 K to that at room temperature is estimated to be less than 1% on the assumption of a typical Debye temperature of ~630 K in M/HEAs,<sup>23</sup> the thermal component is negligibly small at 20 K. This thermal component is approximately proportional to the square of the temperature in the temperature range below the Debye temperature. We plotted  $\overline{\sigma^2}$  as a function of the square of the reduction in the yield strength  $(\tau_{20K} - \tau)^2$ in the inset of Fig. 3. Here,  $\overline{\sigma^2}$  denotes the average value of the Debye-Waller factors in Cr, Co, and Ni  $((\sigma_{Cr}^2 + \sigma_{Ni}^2)/3)$ , and we utilized the values of the yield strength reported in the previous studies.  $^{20,24-26}$  As seen in the figure, the high-temperature reduction in the yield strength correlates with the Debye-Waller factor. At 200 and 293 K, the thermal fluctuation of the lattice not only screens the element dependence of the static disorder but also assists the motion

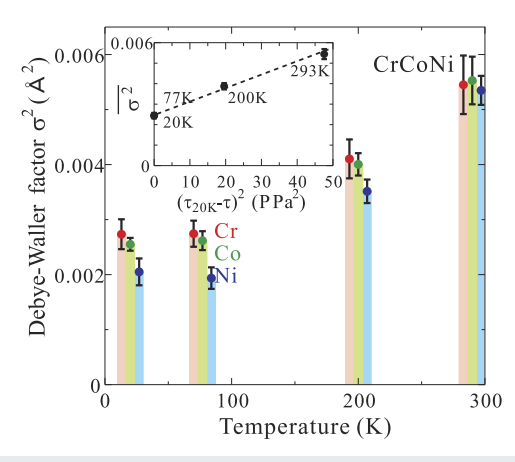


**FIG. 3.** Temperature dependence of the Debye–Waller factors obtained by EXAFS in Cr (red), Co (green), and Ni (blue) of CrCoNi annealed at 773 K for 20 h. For clarity, the data in each element are shifted slightly in the horizontal direction. Inset: Correlation between the averaged Debye–Waller factors  $\overline{\sigma^2}$  and the square of the reduction in yield strength  $(\tau_{20K} - \tau)^2$ . The dashed line is a guide for the eye.

of the dislocation under the stress, leading to a reduction in yield strength.

In summary, we investigated the element dependence of the local disorder in CrCoNi by EXAFS measurement. The local disorder in the Cr site is larger than that in other constituent element sites. Our experimental results are consistent with the reported first-principles calculation, which suggested the large atomic displacement of Cr. The Cr atom is considered a solute-type atom that induces the local disorder. In the temperature region in which the short-range order develops, long-term annealing reduces the differences in local disorder between the constituent elements. This result recalls that the static atomic displacement, which is supposed to be key in tuning the mechanical properties, can be modified by low-temperature annealing.

#### SUPPLEMENTARY MATERIAL

See the supplementary material for the structural parameter in the EXAFS analysis and the comparison between the Debye–Waller factors in the EXAFS of CrCoNi and the Debye–Waller factors in the x-ray diffraction of pure metal Cr and Ni.

The authors thank K. Tanaka, T. Komoda, T. Kawabata, K. Minamoto, and D. Furuya for their valuable discussions. This work was financially supported by the Grant-in-Aid for Scientific Research on Innovative Area "High-Entropy Alloys" (JSPS Grant Nos. 19H05173 and 21H00147), the JSPS KAKENHI (Grant Nos. 19H01851 and 21K03445) in MEXT, Japan, and the Asahi Glass Foundation. The synchrotron radiation experiments were performed at the BL-8B and 12C of the photon factory under the approval of the Photon Factory Program Advisory Committee (Proposal Nos. 2019G660, 2019G679, 2021G669, and 2021G682). This work was carried out, in part, at the Center for Spintronics

Research Network (CSRN), Graduate School of Engineering Science, Osaka University.

#### **AUTHOR DECLARATIONS**

#### **Conflict of Interest**

The authors have no conflicts to disclose.

#### **DATA AVAILABILITY**

The data that support the findings of this study are available within the article and its supplementary material.

#### **REFERENCES**

- <sup>1</sup>J.-W. Yeh, S.-K. Chen, S.-J. Lin, J.-Y. Gan, T.-S. Chin, T.-T. Shun, C.-H. Tsau, and S.-Y. Chang, Adv. Eng. Mater. **6**, 299 (2004).
- <sup>2</sup>B. Cantor, I. T. H. Chang, P. Knight, and A. J. B. Vincent, Mater. Sci. Eng., A 375-377, 213 (2004).
- <sup>3</sup>B. Gludovatz, A. Hohenwarter, D. Catoor, E. H. Chang, E. P. George, and R. O. Ritchie, Science **345**, 1153 (2014).
- <sup>4</sup>R. L. Fleischer, in *The Strengthening of Metals*, edited by D. Peckner (Reinhold Publishing Co., Ltd., New York, 1964).
- <sup>5</sup>R. Labusch, Phys. Status Solidi **41**, 659 (1970).
- <sup>6</sup>I. Toda-Caraballo, Scr. Mater. **127**, 113 (2017).
- <sup>7</sup>C. Varenne, A. Luque, and W. A. Curtin, Acta Mater. 118, 164 (2016).
- <sup>8</sup>N. L. Okamoto, K. Yuge, K. Tanaka, H. Inui, and E. P. George, AIP Adv. 6, 125008 (2016).
- <sup>9</sup>K. Niitsu, M. Asakura, K. Yuge, and H. Inui, Mater. Trans. **61**, 1874 (2020).
- <sup>10</sup> F. X. Zhang, S. Zhao, K. Jin, H. Xue, G. Velisa, H. Bei, R. Huang, J. Y. P. Ko, D. C. Pagan, J. C. Neuefeind, W. J. Weber, and Y. Zhang, Phys. Rev. Lett. **118**, 205501 (2017).
- <sup>11</sup>F. Zhang, Y. Tong, K. Jin, H. Bei, W. J. Weber, A. Huq, A. Lanzirotti, M. Newville, D. C. Pagan, J. Y. P. Ko, and Y. Zhang, Mater. Res. Lett. 6, 450 (2018).
- <sup>12</sup> R. Zhang, S. Zhao, J. Ding, Y. Chong, T. Jia, C. Ophus, M. Asta, R. O. Ritchie, and A. M. Minor, Nature **581**, 283 (2020).
- <sup>13</sup>Q.-J. Li, H. Sheng, and E. Ma, Nat. Commun. **10**, 3563 (2019).
- <sup>14</sup>B. Ravel and M. Newville, J. Synchrotron Radiat. **12**, 537 (2005).
- <sup>15</sup>B. K. Teo, EXAFS: Basic Principles and Data Analysis (Springer, Berlin, 1986).
- <sup>16</sup>S. Torigoe, Y. Ishimoto, Y. Aoishi, H. Murakawa, D. Matsumura, K. Yoshii, Y. Yoneda, Y. Nishihata, K. Kodama, K. Tomiyasu, K. Ikeda, H. Nakao, Y. Nogami, N. Ikeda, T. Otomo, and N. Hanasaki, Phys. Rev. B 93, 085109 (2016).
- <sup>17</sup>S. Torigoe, T. Hattori, K. Kodama, T. Honda, H. Sagayama, K. Ikeda, T. Otomo, H. Nitani, H. Abe, H. Murakawa, H. Sakai, and N. Hanasaki, *Phys. Rev. B* 98, 134443 (2018).
- <sup>18</sup>K. Jin, B. C. Sales, G. M. Stocks, G. D. Samolyuk, M. Daene, W. J. Weber, Y. Zhang, and H. Bei, Sci. Rep. 6, 20159 (2016).
- <sup>19</sup> M. L. Ali, S. Shinzato, V. Wang, Z. Shen, J.-p. Du, and S. Ogata, Mater. Trans. 61, 605 (2020).
- <sup>20</sup>Z. Wu, H. Bei, G. M. Pharr, and E. P. George, Acta Mater. **81**, 428 (2014).
- <sup>21</sup> N. Singh and P. K. Sharma, Phys. Rev. B **3**, 1141 (1971).
- <sup>22</sup>G. Beni and P. M. Platzman, Phys. Rev. B **14**, 1514 (1976).
- $^{\bf 23}$  S. Wang, T. Zhang, H. Hou, and Y. Zhao, Phys. Status Solidi B 255, 1800306 (2018).
- <sup>24</sup>B. Gludovatz, A. Hohenwarter, K. V. S. Thurston, H. Bei, Z. Wu, E. P. George, and R. O. Ritchie, Nat. Commun. 7, 10602 (2016).
- <sup>25</sup>M. Yang, L. Zhou, C. Wang, P. Jiang, F. Yuan, E. Ma, and X. Wu, Scr. Mater. 172, 66 (2019).
- $^{26}$ The value of the yield strength at 20 K was estimated by the interpolation between 4 and 77 K, since the yield strength is saturated below ~77 K.